Experimental study of the frequency repulsion effect

R. F. Gamarra, M. Josebachuili, and P. Zurita
Departamento de Física, "J. J. Giambiagi," F.C.E.y N., Universidad de Buenos Aires, Argentina

S. Gil[a)]
Departamento de Física, "J. J. Giambiagi," F.C.E.y N., Universidad de Buenos Aires, Argentina and Escuela de Ciencia y Tecnología, Universidad Nacional de San Martín, Campus Miguelete, M. de Irigoyen 3100, San Martín (1650), Buenos Aires, Argentina

(Received 11 May 2007; accepted 28 August 2007)

We discuss an experiment on coupled RLC circuits with variable coupling strength. The inductive coupling can be easily varied and measured for different configurations. The experiment allows us to explore the variation of the resonance frequencies as a function of the coupling strength between the oscillators. The system illustrates the effect of eigenfrequency repulsion when an interaction couples different modes of oscillation. The experiment is conceptually simple, and its results can be compared quantitatively with theoretical predictions. © *2007 American Association of Physics Teachers.*
[DOI: 10.1119/1.2787017]

I. INTRODUCTION

The study of coupled oscillators is of interest in many areas of physics and related areas. An interesting and important phenomenon in these systems is the frequency repulsion effect. A system of two coupled oscillators has two natural frequencies or eigenfrequencies.[1] As the coupling strength increases, the lower eigenfrequency decreases and the higher increases; the effect is a "repulsion" between the eigenfrequencies. The quantum mechanical analog of this repulsion effect (level repulsion) is known as the Wigner–von Neumann anticrossing rule,[2] which is important in molecular, atomic, nuclear, and particle physics.[3–5] An interesting example is the ammonia molecule in an electric field.[3] Other examples include the hyperfine splitting of the hydrogen atom in a magnetic field,[3] the Nilsson model for deformed nuclei,[6,7] and the neutrino oscillation between flavors.[8]

There are few experiments that illustrate the consequences of level repulsion.[9,10] The experimental system we will discuss is an inductively coupled RLC circuit. This system is easy to understand by beginning and intermediate students, and the experiment is low cost and readily accessible. The coupling strength can be easily measured and modified in a continuous and convenient way. A simple theoretical model accounts for the experimental data. Previous studies[9] with different experimental setups and techniques lacked the necessary sensitivity and accuracy[9] but paved the way for the present approach.

There are several ways to perform this experiment. We employ a lock-in amplifier.[11] Lock-in amplifiers are versatile and useful instruments and are increasingly used in research and industrial settings. Lock-in amplifiers are particularly useful for detecting small signals of known frequency in the presence of a noisy environment. There have been several developments that have made lock-in amplifiers available to teaching laboratories with modest budgets.[12,13] Although a lock-in amplifier is a useful tool for this experiment, it is not essential and a good oscilloscope could be used instead, at the expense of making the experiment more time consuming and much less sensitive to small signals.

II. THEORETICAL CONSIDERATIONS

The theory of the frequency repulsion effect has been extensively discussed.[3–5] The basic physical process involved in frequency repulsion can be illustrated for two coupled harmonic oscillators. We briefly review the two inductively coupled LC circuits indicated schematically in Fig. 1.

We apply Kirchhoff's law to the circuit of Fig. 1 and obtain

$$\frac{Q_1}{C_1} + L_1\frac{dI_1}{dt} \pm M\frac{dI_2}{dt} = 0, \tag{1}$$

and

$$\frac{Q_2}{C_2} + L_2\frac{dI_2}{dt} \pm M\frac{dI_1}{dt} = 0. \tag{2}$$

Here $Q_k(t)$ and $I_k(t)=dQ_k(t)/dt$ are the charges and the currents in circuits 1 (left) and 2 (right), and M is the mutual inductance coefficient. The different signs for M are related to the relative orientation of the induction coils[14] L_1 and L_2. The condition $M^2 \leq L_1L_2$ must be satisfied.[14] To solve this system of coupled differential equations we assume that

$$Q_k(t) = A_k \exp(i\omega t). \tag{3}$$

We substitute this form into Eqs. (1) and (2), yielding

$$\frac{A_1}{C_1} - L_1A_1\omega^2 \mp MA_2\omega^2 = 0, \tag{4}$$

and

$$\frac{A_2}{C_2} - L_2A_2\omega^2 \mp MA_1\omega^2 = 0. \tag{5}$$

We define

$$\omega_{10}^2 = \frac{1}{L_1C_1} \quad \text{and} \quad \omega_{20}^2 = \frac{1}{L_2C_2}, \tag{6}$$

and cast Eqs. (4) and (5) in the matrix form:

$$\begin{pmatrix} (\omega_{10}^2 - \omega^2) & \mp\dfrac{M}{L_1}\omega^2 \\ \mp\dfrac{M}{L_2}\omega^2 & (\omega_{20}^2 - \omega^2) \end{pmatrix} \begin{pmatrix} A_1 \\ A_2 \end{pmatrix} = 0. \tag{7}$$

 © 2007 American Association of Physics Teachers

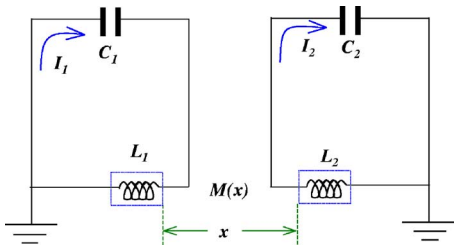

Fig. 1. Inductively coupled LC circuits.

The solution to Eq. (7) differs from the trivial solution $(A_1=A_2=0)$ only if the determinant of this matrix is zero, that is,

$$\begin{vmatrix} (\omega_{10}^2-\omega^2) & \mp\dfrac{M}{L_1}\omega^2 \\ \mp\dfrac{M}{L_2}\omega^2 & (\omega_{20}^2-\omega^2) \end{vmatrix} = (\omega_{10}^2-\omega^2)(\omega_{20}^2-\omega^2) - \frac{M^2}{L_1L_2}\omega^4 = 0. \tag{8}$$

If we define

$$\alpha = \frac{M^2}{L_1L_2}, \tag{9}$$

with $0\leq\alpha\leq 1$, the natural frequencies of the coupled system are

$$\tilde{\omega}^2 = \frac{1}{2(1-\alpha)}[(\omega_{10}^2+\omega_{20}^2) \pm \sqrt{\omega_{10}^4+\omega_{20}^4-2(1-2\alpha)\cdot\omega_{10}^2\omega_{20}^2}]. \tag{10}$$

It follows from Eq. (10) that

$$|\tilde{\omega}_1^2-\tilde{\omega}_2^2| \geq |\omega_{10}^2-\omega_{20}^2|. \tag{11}$$

Equation (11) implies that the difference between the eigenfrequencies in the coupled system is larger than that of the uncoupled case. The ratio $|\tilde{\omega}_1^2-\tilde{\omega}_2^2| \div |\omega_{10}^2-\omega_{20}^2|$ increases monotonically with α and is independent of the sign of coupling strength M.

The quantum analog of this phenomenon is the level repulsion effect.[3–5] A simple explanation of this effect can be given by considering a two level system. Assume that in the absence of interaction there is the Hamiltonian H_0 with eigenenergies E_1^0 and E_2^0:

$$H_0\psi_i^0 = E_i^0\psi_i^0, \quad (i=1,2), \tag{12}$$

where ψ_i^0 is the eigenfunction of H_0 corresponding to the eigenvalue E_i^0. Suppose that an interaction V is introduced that mixes the states 1 and 2 such that

$$\langle\psi_j^0|V|\psi_i^0\rangle = V_0(1-\delta_{j,i}). \tag{13}$$

The perturbed Hamiltonian $H=H_0+V$ has eigenenergies E_i given by[3–5]

$$E_{1,2} = \frac{1}{2}[(E_1^0+E_2^0) \pm \sqrt{(E_2^0-E_1^0)^2+4V_0^2}]. \tag{14}$$

The energy difference has the following property:

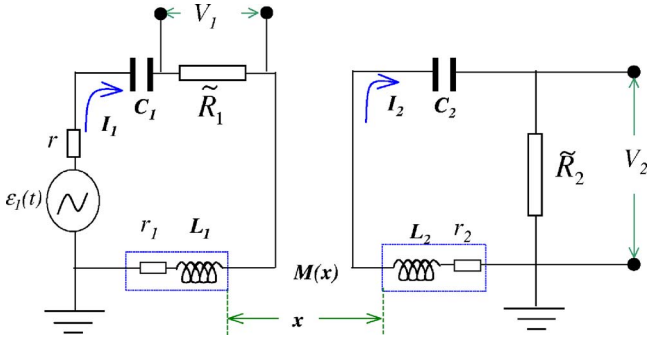

Fig. 2. Inductively coupled RLC circuits. The resistance r is the internal resistance of the AC source, and r_1 and r_2 are the internal resistances of inductors having inductances L_1 and L_2, respectively. The voltage drop in the resistances of the primary and secondary circuits is measured directly by the lock-in amplifier. V_i is the voltage drop in the resistance $\tilde{R}_i$ and is used to monitor the currents in each network.

$$|E_2-E_1| = \sqrt{(E_2^0-E_1^0)^2+4V_0^2} \geq |E_2^0-E_1^0|. \tag{15}$$

Equation (15) indicates that the energy difference increases monotonically with the magnitude of the coupling strength V_0.[3–5]

III. THE EXPERIMENT

We built a coupled classical RLC resonator (see Figs. 2 and 3). Here x is the axial distance between the two coils with $x=0$ corresponding to the two coils being side by side. Figure 3 is the physical realization of the circuit shown in Fig. 2. The presence of the resistances in the circuits has a double origin. Inductances always have some internal resistance, and the external resistances $\tilde{R}_i$ are useful for monitoring the responses (currents) of the circuits. In a single RLC (series) circuit the resonance frequency coincides with the natural frequency.[14] To characterize the natural frequencies of a coupled RLC circuit we built an apparatus, illustrated in Fig. 3, that allowed us to study the resonance curve in this circuit. The parameters of the two coupled RLC circuits are given in Table I. The internal resistance of the AC source (function generator) is r; the internal resistances of the inductances L_1 and L_2 are r_1 and r_2, respectively. We denote by

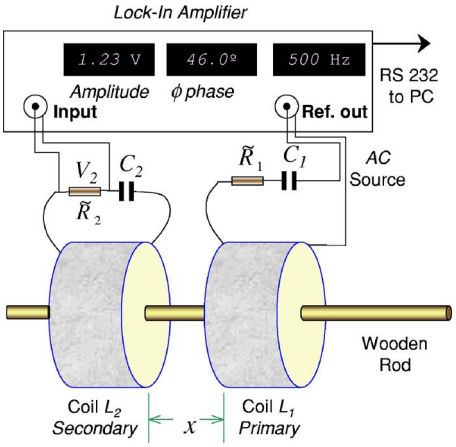

Fig. 3. Schematic of the experimental setup. The two coils move along a wooden rod. Here x is the separation between the coils. An AC source is connected to the primary circuit.

Table I. Values of the parameters used. The second column shows the values of the parameters obtained by direct measurements. The third column shows the results obtained from a fit of the data, as illustrated in Fig. 6. In this case the model provides only the total resistance of the circuit.

	Direct measurement	From best fit to the model
$\tilde{R}_1$	15±1 Ω	
$\tilde{R}_2$	7±1 Ω	
r	50±2 Ω	
r_1	18±1 Ω	
r_2	19±1 Ω	
R_1	83±3 Ω	90±4 Ω
R_2	26±3 Ω	31±4 Ω
L_1	32.4±0.2 mH	32±5 mH
L_2	33.5±0.2 mH	34±5 mH
C_1	99.1±0.2 nF	99±7 nF
C_2	108±0.2 nF	108±3 nF

$\tilde{R}_1$ and $\tilde{R}_2$ the external resistors in the primary and secondary circuits and the total resistance in these circuits by R_1 and R_2. The voltage drops across the external resistances, V_1 and V_2, are used alternatively as input for the lock-in amplifier. The currents in the primary and secondary circuit are equal to the ratios $V_1/\tilde{R}_1$ and $V_2/\tilde{R}_2$, respectively. The internal oscillator of the lock-in amplifier is used to power the primary loop.

The values of all the parameters of the circuit were measured independently, including the internal resistance of the coils and the internal resistance of the AC power supply. The coils were made of copper wires gauge #26 (diameter =0.4 mm) of 1040 turns. The coils had an internal diameter of 2.5 cm, an external diameter of 5.2 cm, and a width of 2 cm. The two coils could snugly move over a common wooden rod. This arrangement allowed us to conveniently varying the distance between the coils and consequently the mutual induction M (coupling strength) of the system.

The value of M as a function of the distance x between the two coils was determined independently. For this purpose we measured the induced voltage in the secondary inductance L_2 alone with no other component connected. From the definition of M we have[14]

$$\varepsilon_2 = -M\frac{dI_1}{dt}. \tag{16}$$

Because we excited the circuit with a sinusoidal signal of frequency ω_0, the amplitude of the induced emf ε_2^0 is given by

$$\varepsilon_2^0 = -M\omega_0\frac{V_1^0}{\tilde{R}_1}. \tag{17}$$

Equation (17) allows us to obtain M from measurements of the amplitude of the voltage drop V_1^0 across $\tilde{R}_1$ and the amplitude of the induced emf in the secondary inductance. This procedure was used to determine how M varies with x. After we obtained M for different values of x, we measured the voltages drops across both $\tilde{R}_1$ and $\tilde{R}_2$ in the same geometry we used for M. In this way we obtained V_1^0 and V_2^0 as a function of the frequency.

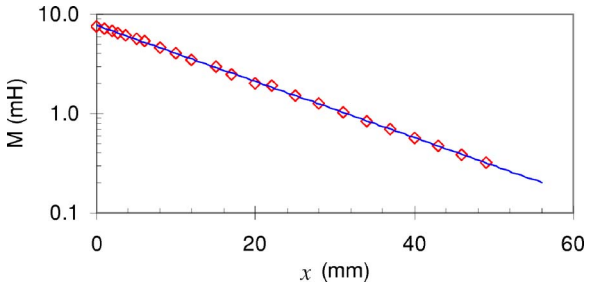

Fig. 4. Experimental results for the mutual inductance M as a function of the separation x. The diamond symbols are the results for M obtained by direct measurements of x. The continuous line is an empirical fit to the data using an exponential function.

To characterize the frequency response of our coupled oscillator, we used a digital lock-in amplifier SR830 controlled by a computer. This arrangement allowed us to measure the magnitude of the current for each excitation frequency. The computer allowed us to sweep the excitation frequency between 1 to 40 kHz at the preset step of 500 Hz. As indicated in Fig. 3, the reference output of the lock-in amplifier was used to feed the circuit (AC source). Further technical details of this experiment are available.[15]

IV. RESULTS AND DISCUSSION

In Fig. 4 we show the variation of M as a function of x and an empirical fit to the data. The diamonds represent the values obtained by the measurement of the emf in the secondary self inductance.

Figure 5 shows the results of the response of the primary circuit, that is, the amplitude of the current in the primary circuit $V_1/\tilde{R}_1$ for different values of x. For a large separation of the coils (uncoupled system) we observe the response of the primary circuit alone. By adjusting the parameters of the model to the experimental results, it is possible to obtain the parameters of the system. In Table I the values thus obtained are compared to those obtained by direct measurements of the individual components. The values agree within a few percent, indicating the consistency of the methods employed.

In Fig. 6 we show the response of the secondary circuit using V_2 as the input for the lock-in amplifier for different values of x. We also include in Fig. 6 the response of the secondary circuit when the system is uncoupled. To obtain

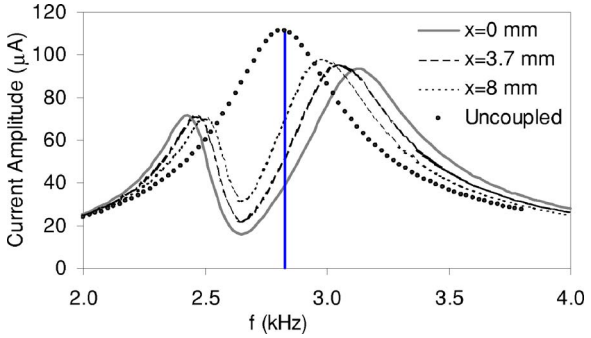

Fig. 5. The observed current amplitude in the primary circuit as a function of frequency for different separations between the coils. The frequency separation of the maxima of these curves increases for smaller distances, that is, stronger coupling.

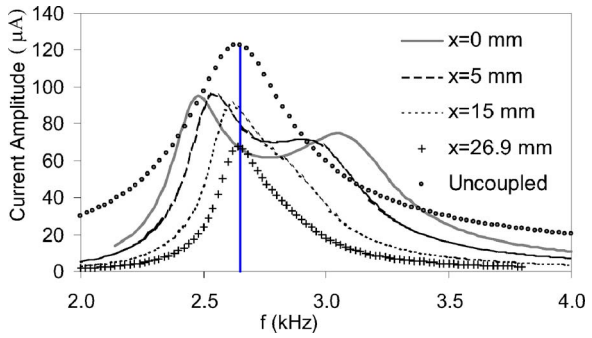

Fig. 6. The observed current amplitude in the secondary circuit as a function of frequency for different separations between the coils. As in Fig. 5, the frequency separation of the maxima increases for smaller distances.

the resonance curve for this case we excited the secondary circuit (alone) with the reference output of the lock-in amplifier. The broadening in the uncoupled curve is due to the presence of the internal resistance of the function generator ($r \approx 50\ \Omega$) used to excite the secondary circuit. Note that as the coupling decreases (x increases), the amplitude of the signal in the secondary diminishes. The larger signal observed in the uncoupled case is a consequence of the direct way we used to excite this system. Despite these differences, the frequencies of the maxima in the uncoupled and weakest coupling cases coincide as expected.

Figures 5 and 6 show that when the coupling between the two systems is nonzero, there is a bimodal resonance curve. The positions of the maxima separate for smaller distances between the coils (larger coupling strength) in agreement with the theoretical expectation, Eq. (10).

In Fig. 7 we present the results of the current amplitude for the primary and secondary circuits for $x=0$. The symbols indicate the measured current amplitude in the primary and secondary circuits (see Fig. 2). We also plotted in Fig. 7 the corresponding theoretical prediction from Eqs. (A10) and (A11). Figure 7 shows how well the theory reproduces the experimental data. The adjustable parameters of the model are the values of M, R_i, L_i, and C_i. The values of these parameters obtained from this fit are given in the third column of Table I. The fit of the model to the data provides another way of determining M and the other parameters. As Table I indicates, the results of these parameters thus obtained are consistent with those obtained from direct measurements.

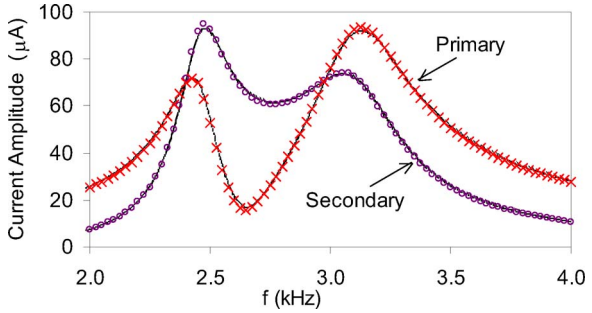

Fig. 7. The observed current amplitude as a function of the frequency in the primary (crosses) and secondary (circles) circuits for $x=0$. The continuous lines are fits to the data using Eq. (A10) with the mutual induction coefficient $M(x)$ as the only adjustable parameter. The values of M obtained for each value of x are shown in Fig. 4.

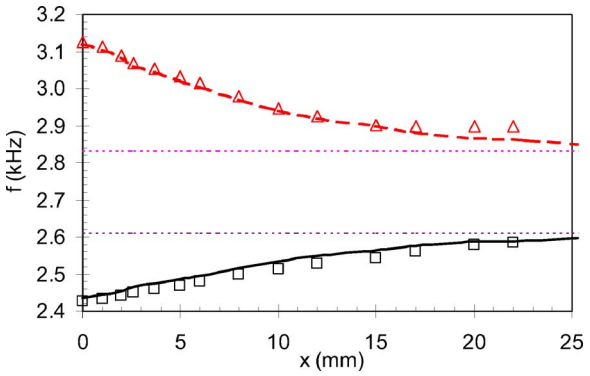

Fig. 8. Observed maximum response frequencies as a function of x. The heavy lines are the result of Eq. (10). The dotted horizontal lines indicate the uncoupled eigenfrequencies. The square symbols and triangles represent the eigenfrequencies (frequencies of the maxima in the secondary circuit of Fig. 6).

Figure 8 shows that as the coupling strength increases, the repulsion effect is enhanced (that is, the difference between the eigenfrequencies increases), in agreement with Eq. (10). For large separations between the coils the eigenfrequencies converge to the uncoupled values. The theoretical result, Eq. (10), is indicated by the heavy lines.

V. CONCLUSIONS

The experimental setup is a simple way to study the basic characteristics of coupled oscillators with variable coupling strength. The effect of eigenfrequencies repulsion is readily observable. The model provides an excellent description of the data. The experiment and the model can be generalized to several coupled oscillators. Finally, the experiment provides an instructive and useful application of the lock-in amplifier for studying interesting phenomena. A recent submission to this journal has been brought to our attention by the Editor.[17] It studies the same system from a somewhat different perspective. Their findings are in keeping with the effect described in our study.

ACKNOWLEDGMENTS

The authors would like to express their acknowledgement of the other students who have explored the physics of coupled circuits with different experimental techniques. They also express their gratitude to Prof. Carlos Acha for his assistance in the setting and programming of the lock-in amplifier and to the valuable comments and suggestions made by Dr. E. Batista and Prof. C. Grosse. We are also grateful to Dr. A. Schwint for a careful reading of the manuscript.

APPENDIX: FORCED COUPLED RLC CIRCUITS

Consider the circuit in Fig. 2. An AC source powers the left network (primary). We characterize the voltage generated by the AC power source as $v_1(t)=V_{10}\exp(-i\omega t-\phi)$, where V_{10} is the amplitude of the signal, ω is the angular frequency, and ϕ is the phase difference with the current in the primary. If we measure the voltage drop across the resistances $\tilde{R}_1$ and $\tilde{R}_2$, we can monitor the current in each loop. In the following R_1 and R_2 are the total resistance of the pri-

mary and secondary loops, including the internal resistance of the source (primary) and the resistance of the inductances.

To solve this circuit we assume that[14,16]

$$I_1(t) = I_{10}\exp(i\omega t) \quad \text{and} \quad I_2(t) = I_{20}\exp(i\omega t + \varphi_2). \tag{A1}$$

The complex impedances of the left and right loop are respectively:[14,16]

$$Z_1(\omega) = R_1 + i(L_1\omega - 1/\omega C_1) = R_1 + iX_1(\omega), \tag{A2}$$

and

$$Z_2(\omega) = R_2 + i(L_2\omega - 1/\omega C_2) = R_2 + iX_2(\omega). \tag{A3}$$

According to Kirchhoff's laws we have

$$V_{10}\exp(i\omega t - \phi) = Z_1(\omega)I_1(t) - Mi\omega I_2(t), \tag{A4}$$

and

$$Z_2(\omega)I_2(t) - Mi\omega I_1(t) = 0. \tag{A5}$$

The solution for $i_2(t)$ yields:

$$V_{10}\exp(i\omega t - \phi) = I_1(t)(Z_1(\omega) + \omega^2 M^2 Z_2(\omega)) = I_1(t)Z_1'(\omega), \tag{A6}$$

with

$$Z_1'(\omega) = \left(R_1 + \frac{\omega^2 M^2 R_2}{R_2^2 + X_2^2}\right) + i\left(X_1 - \frac{\omega^2 M^2 X_2}{R_2^2 + X_2^2}\right) = R_e + iX_e(\omega). \tag{A7}$$

The solutions for I_1 and I_2 are

$$I_1(t) = I_{10}\exp(i\omega t) = V_{10}\exp(i\omega t - \phi)(Z_2(\omega)(Z_1(\omega)Z_2(\omega) + \omega^2 M^2)), \tag{A8}$$

and

$$I_2(t) = I_{20}\exp(i\omega t + \varphi_2) = iV_{10}\exp(j\omega t - \phi) \times (M\omega(Z_1(\omega)Z_2(\omega) + \omega^2 M^2)). \tag{A9}$$

The magnitude of the current amplitudes, I_{10} and I_{20}, can be written as

$$I_{10} = V_{10}\left(\frac{\sqrt{R_2^2 + X_2^2}}{D}\right) \quad \text{and} \quad I_{20} = V_{10}\left(\frac{\omega M}{D}\right), \tag{A10}$$

with

$$D^2 = [(R_1R_2 - X_1X_2 + \omega^2M^2)^2 + (R_1X_1 + R_2X_1)^2]. \tag{A11}$$

Equations (A19) and (A11) are the stationary solutions of the coupled circuit and can be directly compared with the results of our measurements. The continuous lines in Figs. 6 and 10 were obtained using Eqs. (A10) and (A11).

[a]Author to whom correspondence should be addressed; Electronic mail: sgil@unsam.edu.ar

[1] H. Goldstein, C. Poole, and J. Safko, *Classical Mechanics* (Addison-Wesley, Reading, MA, 2001), 3rd ed., Chap. 6.

[2] J. von Neumann and E. Wigner, "Über das Verhalten von Eigenwerten bei adiabatischen Prozessen," Z. Phys. **30**, 467–470 (1929).

[3] R. P. Feynman, R. B. Leighton, and M. Sands, *Feynman Lectures on Physics* (Addison-Wesley, Reading, MA, 1970), Vol. 3, Chaps. 9–11.

[4] C. Cohen-Tannoudji, B. Diu, and F. Laloe, *Quantum Mechanics* (John Wiley & Sons, NY, 1977), Vol. 1, Chap. 4.

[5] W. Frank and P. von Brentano, "Classical analogy to quantum mechanical level repulsion," Am. J. Phys. **62**(8), 706–709 (1994).

[6] P. Ring and P. Schuck, *The Nuclear Many-Body Problem* (Springer-Verlag, NY, 1980).

[7] A discussion of the Nillson model can be found at ⟨www.phys.jyu.fi/research/gamma/publications/ptgthesis/node7.html⟩.

[8] E. Sassaroli, "Neutrino oscillations: A relativistic example of a two-level system," Am. J. Phys. **67**(10), 869–875 (1999).

[9] H. A. Atwater, "Laboratory exercises in classical electromagnetic field theory," Am. J. Phys. **36**(8), 672–682 (1968).

[10] C. L. Garrido Alzar, M. A. G. Martinez, and P. Nussenzveig, "Classical analogy of electromagnetically induced transparency," Am. J. Phys. **70**(1), 37–41 (2002).

[11] J. H. Scofield, "Frequency-domain description of a lock-in amplifier," Am. J. Phys. **62**(2), 129 (1994).

[12] S. K. Sengupta, J. M. Farnham, and J. E. Whitten, "A simple low-cost lock-in amplifier for the laboratory," J. Chem. Educ. **82**(9), 1400–1401 (2005).

[13] National Instruments, "Creating a lock-in amplifier with LabVIEW," ⟨zone.ni.com/devzone/cda/tut/p/id/4026⟩.

[14] J. R. Reitz, J. R. Milford, and R. W. Christy, *Foundations of Electromagnetic Theory*, 4th ed. (Addison-Wesley, Reading, MA, 1993), Chaps. 11 and 13.

[15] See EPAPS Document No. E-AJPIAS-75-017711 for more details about our experiment (including photographs) and the Excel file used to fit the experimental results. The files can also be obtained at (www.fisicarecreativa.com). This document can be reached through a direct link in the online article's HTML reference section or via the EPAPS homepage (www.aip.org/pubservs/epaps.html).

[16] B. Kurrelmeyer and W. H. Mais, *Electricity and Magnetism* (Van Nostrand, Princeton, NJ, 1967), pp. 351–379.

[17] M. J. Schauber, S. A. Newman, L. R. Goodman, I. S. Suzuki, and M. Suzuki, "Measurement of mutual inductance from frequency dependence of impedance of AC coupled circuits using a digital dual-phase lock-in amplifier," Am. J. Phys. (accepted).